

UC Irvine

UC Irvine Previously Published Works

Title

Near-canopy horizontal concentration heterogeneity of semivolatile oxygenated organic compounds and implications for 2-methyltetrols primary emissions

Permalink

<https://escholarship.org/uc/item/6jh7c4b9>

Journal

Environmental Science Atmospheres, 1(1)

ISSN

2634-3606

Authors

Ye, Jianhuai
Batista, Carla E
Guimarães, Patricia C
[et al.](#)

Publication Date

2021-01-28

DOI

10.1039/d0ea00006j

Peer reviewed

1 *Major category:* Physical Sciences, *Minor category:* Atmospheric, and Planetary Sciences

2 **Title: Intermediate-scale horizontal isoprene concentrations in the near-canopy forest**

3 **atmosphere and implications for emission heterogeneity**

4 Carla E. Batista,^{1,2†} Jianhuai Ye,^{3†*} Igor O. Ribeiro,^{1,2} Patricia C. Guimarães,^{1,2} Adan S. S.

5 Medeiros,^{1,2,4} Rafael G. Barbosa,² Rafael L. Oliveira,² Sergio Duvoisin Jr.,^{1,2} Kolby J. Jardine,⁵

6 Dasa Gu,⁶ Alex B. Guenther,⁶ Karena A. McKinney,⁷ Leila D. Martins,⁸ Rodrigo A. F. Souza,^{1,2*}

7 Scot T. Martin,^{3,9*}

8 ¹Post-graduate Program in Climate and Environment, National Institute of Amazonian Research
9 and Amazonas State University, Manaus, Amazonas, 69060-001, Brazil

10 ²School of Technology, Amazonas State University, 69065-020, Manaus, Amazonas, Brazil

11 ³School of Engineering and Applied Sciences, Harvard University, Cambridge, Massachusetts,
12 02138, USA

13 ⁴Advanced Study Center at Tefé, Amazonas State University, 69553-100, Tefé, Amazonas,
14 Brazil

15 ⁵Climate and Ecosystem Sciences Division, Earth Science Division, Lawrence Berkeley National
16 Laboratory, Berkeley, California, 94720, USA

17 ⁶Department of Earth System Science, University of California, Irvine, California, 92697, USA

18 ⁷Department of Chemistry, Colby College, Waterville, Maine, 04901, USA

19 ⁸Department of Chemistry, Federal University of Technology-Paraná, Av dos Pioneiros, 3131,
20 86047-125, Londrina, Paraná, Brazil

21 ⁹Department of Earth and Planetary Sciences, Harvard University, Cambridge, Massachusetts,
22 02138, USA

23 Submitted March 2019 to *Proceedings of the National Academy of Sciences of the United States*
24 *of America*

25 †These authors contributed equally to this study.

26 *Correspondence to: Scot T. Martin (scot_martin@harvard.edu), Rodrigo A. F. Souza
27 (souzaraf@gmail.com), and Jianhuai Ye (jye@seas.harvard.edu)

28 **Abstract**

29 The emissions, deposition, and chemistry of volatile organic compounds (VOCs) are
30 thought to be influenced by underlying landscape heterogeneity at intermediate horizontal scales
31 of several hundred meters across different forest sub-types within a tropical forest. Quantitative
32 observations and scientific understanding at these scales, however, remain lacking, in large part
33 due to a historical absence of canopy access and atmospheric observational approaches. Herein,
34 horizontal heterogeneity in VOC concentrations in the near-canopy atmosphere was examined by
35 sampling from an unmanned aerial vehicle (UAV) flown over contiguous plateau and slope
36 forests separated horizontally by several hundred meters in central Amazonia during morning
37 and early afternoon periods of the wet season of 2018. Unlike terpene concentrations, the
38 isoprene concentrations in the near-canopy atmosphere over the plateau forest were 60% greater
39 than those over the slope forest. A gradient transport model with these data sets constrains
40 isoprene emissions as 220% to 330% greater for the former as compared to the latter, which is in
41 contrast to the homogeneous emissions of 0% difference implemented in most present-day
42 models. Quantifying VOC concentrations, emissions, and other processes at intermediate
43 horizontal scales is essential for understanding the ecological and Earth system roles of VOCs
44 and representing them in climate and air quality models.

45 Keywords: isoprene emissions, landscape heterogeneity, intermediate horizontal scales, Amazon
46 tropical forest, UAV measurements

47 **Significance Statement**

48 Unquantified intermediate-scale heterogeneity in VOC emissions over Amazonia may be
49 a key contributor to the observed discrepancy between measured and modeled VOC
50 concentrations, but in situ measurements with which to investigate the possibility have been
51 lacking. The measurements presented herein quantify horizontal VOC concentration gradients in
52 the near-canopy atmosphere across different forest sub-types at the intermediate scale of several
53 hundred meters. **The results suggest that** there are biases in both top-down estimates, based on
54 satellite or aircraft measurements that are too coarse to compare with specific locations, and
55 bottom-up approaches, based on leaf or tower measurements that are difficult to extrapolate to
56 larger domains. The results demonstrate how observations collected by UAV-enabled
57 technologies fill a missing niche among leaf-level, tower, aircraft, and satellite scales.
58 Information at this previously unavailable scale is needed for accurate understanding and
59 predictions in evolving forests under climate stress.

60 **Introduction**

61 Volatile organic compounds (VOCs) emitted from forests have important roles in
62 signaling among plants, animals, insects, and microbes, ecosystem functioning and health, and
63 atmospheric chemistry and climate (1, 2). Tropical forests are the major global VOC source but
64 are comparatively less studied and understood than their temperate and boreal counterparts (3).
65 Tropical forest landscapes can have great heterogeneity and many forest sub-types at scales of
66 100's of meters (i.e., intermediate horizontal scales) (4, 5). In central Amazonia, rolling hills
67 underlying the tropical forest north of the Amazon River give rise to plateaus interspersed by
68 water-logged valleys, all dissected by streams and rivers and joined by sloped regions, at scales
69 of hundreds of meters. Myriad forest sub-types and biodiversity result across this intermediate
70 scale for reasons of water, sunlight, and soil, among other factors and variations (6, 7).

71 The landscape variability at intermediate scales is thought to be associated with
72 variability in VOC emissions at the same scale (8). For any VOC, some tropical forest sub-types
73 can have high emissions of that VOC whereas other sub-types can exhibit low emissions or
74 pockets of net deposition, even as the forest as a whole emits in net. This emerging view of a
75 heterogeneous patchwork of VOC emissions and deposition has important implications for
76 interpreting results of earlier studies that have largely reported VOC observations from single
77 locations, such as tower sites, with no information on the surrounding horizontal heterogeneity in
78 VOC emissions and deposition. Atmospheric chemical transport models also do not accurately
79 simulate VOC oxidation over tropical forests (9), and process-level models such as large-eddy
80 simulations suggest that non-uniform VOC emissions from different forest sub-types can be one
81 possible explanation (10-12). Measurements of VOC variability over the forest sub-types are

82 needed to investigate this possibility as well as to improve predictive capabilities for models of
83 emissions and reactive chemistry over these landscapes.

84 Topography is often a first surrogate of landscape variability and thus also of VOC
85 emissions, especially in Amazonia (13, 14). Contributing factors tying topography to forest sub-
86 type are variations in elevation, slope, aspect, drainage, soil type, and microclimate, among
87 others, that determine forest species composition and diversity. Flood-free plateau forest grows
88 on the tops rolling hills, and over 200 species are routinely identified in inventories (15). The
89 soils are strongly leached, with low natural fertility and high acidity. By comparison, valley
90 forests are populated by plants adapted to richer, waterlogged soils and wetlands. More than 100
91 species are typically identified in inventories (15). Slope forests have a mix of valley and plateau
92 plant families. Estimates are on the order of 10,000 distinct tree species across Amazonia (5, 16).

94 Herein, results are reported for investigating the heterogeneity of isoprene concentrations
95 in the near-canopy atmosphere over contiguous plateau, slope, and valley forest sub-types in
96 central Amazonia during the wet season of 2018. Isoprene is the non-methane VOC emitted in
97 greatest quantities by land surfaces on Earth, as represented in the *Model of Emissions of Gases
98 and Aerosols from Nature* (MEGAN) (3). One estimate is that isoprene emissions alone represent
99 70% of total VOCs emitted by plants globally into the atmosphere (17). Leading models such as
100 MEGAN and others, however, are not presently able to predict emissions heterogeneity at the
101 intermediate horizontal scales across forests, even as differences are thought to exist, in large part
102 because of the absence of historical measurement platforms and data sets. For investigation of
103 forest sub-types at intermediate scales without disturbance of the underlying landscape, chemical
104 sampling and sensing by use of unmanned aerial vehicles (UAVs or “drones”) represents an

105 emerging frontier in atmospheric chemistry (18). Data sets of isoprene concentration were
106 collected at intermediate scales by use of the UAV, and relative emission differences were
107 inferred by use of a gradient transport model constrained to the measured heterogeneity in
108 concentration **above different forest sub-types**.

109 **Results**

110 **Different forest sub-types.** The UAV collected samples for two different locations above the
111 Adolfo Ducke Forest Reserve (hereafter, “Ducke Reserve”) in central Amazonia across four
112 weeks during the wet season from February 20 to March 15, 2018. The Ducke Reserve (10 km ×
113 10 km) is located on the northern outskirts of Manaus, Brazil, in central Amazonia. Established
114 in 1963, the reserve is recognized as a globally important site for the study of tropical forests (6,
115 14, 19). A tower (“MUSA” tower; 3.003° S, 59.940° W) is located within the Manaus Botanical
116 Gardens (MUSA) of the reserve (Figure 1) (see Materials and Methods). Valley and plateau
117 regions in the tower vicinity are approximately 50 m and 120 m above sea level (asl),
118 respectively, and they are joined by sloped regions.

119 Biodiversity in Ducke Reserve is well characterized by tree inventory surveys. The plant
120 species and occurrence in the reserve has three major forest classifications, described as valley,
121 slope, and plateau forest sub-types (13-15, 20). These forest sub-types are represented in gray,
122 brown, and green in Figure 1. Valley forest occurs along the sandy banks of streams. Flooding is
123 frequent, and the sediment mixes with the forest litter. Canopy height varies from 20 to 35 m.
124 Plateau forest grows in the highest areas in well-drained yet nutrient-poor clay soil. Canopy
125 height ranges from 25 to 35 m. Emergent trees can reach 45 m. Slope forest dissects the
126 landscape, bridging between the valley and plateau forests. It is characterized by clay soils in the

127 higher reaches of the slopes and sandy-loam soils in the lower parts. Canopy height ranges from
128 25 to 35 m. Another important forest classification at Ducke Reserve, which is interspersed
129 among these major topography-based classifications, is campinarana. It grows on extremely
130 nutrient-poor, poorly drained, white quartz sandy regions. Canopy height varies between 15 and
131 25 m.

132 Ribeiro et al. (20) presented information on the prevalent plant species in each of the
133 forest sub-types at Ducke Reserve, as summarized in **Table S1**. The MUSA forestry staff
134 inspected the actual plant species at locations A and B at the time of UAV flights, and the species
135 were identified as consistent with the inventory of Ribeiro et al. Some important families include
136 *Arecaceae* (commonly referred to as palm trees), *Caryocaraceae*, *Clusiaceae*, *Fabaceae*
137 (legumes), *Lecythidaceae*, *Meliaceae*, *Mimosaceae* (specialized legumes), *Rapataceae*,
138 *Solanaceae* (nightshades), and *Sapotaceae*. The species that grow in abundance are distinct for
139 each forest sub-type (**Table S1**). The photographs shown in Figure 2 of the slope and plateau
140 forests at locations A and B highlight differences in forest composition at the two locations.

141 **Concentrations in near-canopy atmosphere.** The UAV was launched and recovered from a
142 platform atop the MUSA tower (3.0032° S, 59.9397° W; inset picture of Figure 1) (see Materials
143 and Methods). The longitude-latitude point of the MUSA tower is referred to as location A
144 herein. The UAV flew 711 m to 2.997° S and 59.936° W. This longitude-latitude point is
145 referred to as location B in the study. Locations A and B were located over plateau and slope
146 forest sub-types, respectively. The UAV hovered over the canopy at location B and sampled
147 VOCs. An automated sampler, mounted to the UAV, collected the VOC samples in cartridges
148 (21). Simultaneous VOC sampling took place on the tower platform at location A. All samples

149 were analyzed off-line by gas chromatography. For locations A and B, samples were collected
150 cumulatively in 4 different cartridge tubes across a week for 20 min of sampling within each
151 hour of 09:00-10:00, 10:10-11:10, 11:20-12:20, and 12:30-13:30 (local time; 4 h earlier relative
152 to UTC). This approach captured daily trends while ensuring sufficient material for chemical
153 analysis. Four composite samples were collected each week for a total of four weeks over each
154 location, resulting in a total of 32 samples.

155 Many compounds were identified in the collected samples, including isoprene, α -pinene,
156 β -pinene, nine other monoterpenes, β -caryophyllene, and three other sesquiterpenes, together
157 representing a progressive set of C₅, C₁₀, and C₁₅ compounds (Figures S1 and S2). After emission
158 into the atmosphere, these and other VOCs undergo atmospheric mixing and dilution as well as
159 reactive chemical loss. An upward trend is common in the concentrations from morning to noon
160 (3), which can be explained by increasing solar irradiance and temperature (Figure S1). Enzyme
161 activity increases with temperature, and electron transport increases with sunlight until
162 saturation, resulting in a tendency for increases in isoprene and many other VOC emissions from
163 plants and consequently increases in atmospheric concentrations, balanced against atmospheric
164 dilution and chemical loss (22).

165 The isoprene concentrations were consistently higher over the plateau forest compared to
166 over the slope forest. The mean weekly isoprene concentrations above the slope forest ranged
167 from 1.0 to 3.3 ppb (Table S2). The mean concentrations above the plateau forest ranged from
168 2.9 to 4.9 ppb. The mean weekly differences for isoprene concentration over the slope compared
169 to over the plateau forest ranged from 1.5 to 2.7 ppb. For the overall data set, the mean isoprene
170 concentration was 2.4 ppb over the slope forest, which can be compared to 4.4 ppb over the
171 plateau forest, representing an increase of +80% for the latter. The calculated probability (p

172 value) for a two-way ANOVA analysis in location and time is < 0.001 for the null hypothesis
173 that the two sets of isoprene concentrations were the same over locations A and B (Table S3). An
174 implication is that measurements from a single tower placed at either location A or location B
175 would have significant bias if taken as representative of the regional area of Ducke Reserve.

176 The observed isoprene concentrations can be compared to previous reports throughout
177 Amazonia (Section S1 and Table S4). The reported concentrations range from <1 ppb to 27 ppb,
178 in part reflecting the heterogeneity of tropical forests. The mean observed concentrations of 2.4
179 ppb and 4.4 ppb for locations A and B thus lie within the literature range reported for Amazonia.

180 The ratio of the isoprene concentration to the α -pinene concentration is plotted in Figure 3.
181 α -Pinene is typically the monoterpene emitted in largest quantities by the forest. Unlike isoprene
182 concentrations, the α -pinene concentrations and time variability were similar over the plateau
183 and slope forests (Figure S1). The p value was 0.61 for the null hypothesis that the two sets of α -
184 pinene concentrations were the same over location A and location B (Table S3). An advantage of
185 the concentration ratio, compared to the isoprene concentration alone, is mitigation of some
186 possible confounding factors related to differences in transport and reactive loss to locations A
187 and B compared to differences in emissions from forest sub-types at locations A and B. Plots for
188 the isoprene concentration alone, however, have the same major features as Figure 3 (cf. Figures
189 S1 and S2). The isoprene-to- α -pinene concentration ratio over the plateau and slope forests is
190 plotted in the four panels of Figure 3 for the four weeks of sampling. Across 09:00 to 13:30, the
191 mean weekly ratios above the slope forest ranged from 11.4 to 23.7. The ratios above the plateau
192 forest ranged from 27.1 to 42.1. These comparative ratios thus also suggest significantly higher
193 emissions of isoprene by the plateau forest compared to by the slope forest given that the α -
194 pinene concentrations had similar values over the two forest sub-types.

195 **Discussion**

196 Isoprene is emitted across the horizontal extent of the forest as myriad point emissions
197 from **the leaves of individual plants**, and isoprene concentration at the location of UAV sampling
198 in the atmosphere represents the sum of the contribution of each of these point emissions. After
199 being released from a plant, the emitted isoprene is subject to convection in the vertical,
200 advection in the horizontal, and atmospheric chemical reaction (loss) during transport to the
201 location of sampling. Therefore, forest emissions that are directly underlying the point of UAV
202 sampling, as well as forest emissions that are farther afield and delivered to the point of sampling
203 by regional atmospheric transport, affect the isoprene concentration at the location of UAV
204 sampling. Dispersion and reactive loss of isoprene occur between emission at the source region
205 and arrival at the UAV receptor location. Taking these factors into account is required to relate
206 the observed differences in isoprene concentrations at locations A and B to possible differences
207 in the emissions of the underlying forest sub-types.

208 A two-dimensional continuity equation for isoprene concentration can be written, as
209 follows:

$$\frac{\partial C}{\partial t} = -u \frac{\partial C}{\partial x} + K \frac{\partial^2 C}{\partial z^2} + R \quad (1)$$

211 This equation is called a gradient transport model in the flux literature, which is one form of a
212 Reynolds-averaged Navier-Stokes equation (23, 24). The equation simplifies the lower part of
213 the atmosphere as an incompressible fluid at constant pressure **and takes into consideration of**

214 **longitudinal advection** ($-u \frac{\partial C}{\partial x}$), **vertical convection** ($K \frac{\partial^2 C}{\partial z^2}$), **and chemistry** (R). Symbols in

215 the equation include the isoprene concentration $C(x,z;t)$, time t , the longitudinal wind speed u , the
216 eddy diffusion coefficient K , and the reaction rate R , all within a two-dimensional coordinate
217 scheme of distance x and height z . Compared to the longitudinal advection x in the direction of
218 the wind and the vertical convection z in turbulent eddies, transverse mixing y is small in the
219 domain considered for the prevailing wind speeds [ref](#). Therefore, this process is omitted from the
220 model. The local upslope and downslope transport are also omitted from the model due to
221 insignificant differences in the Bowen ratio between plateau and slope forest sub-types [ref](#).

222 Parameter values and data sources for use in Equation 1 are listed in [Table S5](#). Wind
223 speed and direction at tower height were measured. For the altitude of UAV sampling, the wind
224 speed was estimated using a standard relationship (Section S2). Isoprene during mid-morning
225 hours over the tropical forest reacts dominantly with OH and O₃, giving rise to the formulation of
226 reactive chemical loss: $R = - (k_{\text{ISOP+OH}} [\text{OH}] + k_{\text{ISOP+O}_3} [\text{O}_3]) C$, in which the bimolecular rate
227 constant $k_{\text{ISOP+OH}}$ for reactive loss of isoprene with OH and the constant $k_{\text{ISOP+O}_3}$ for loss with O₃
228 are represented. The chemical lifetime τ is given by C/R . The notation of [OH] and [O₃]
229 represents the concentrations of OH and O₃, respectively. Emissions, given by aE where a is a
230 relative emission factor and E is a baseline emission factor, represent a flux boundary condition
231 at $z = 0$ for Equation 1. Other boundary conditions and initial conditions of Equation 1 are
232 presented in Section S2. Possible variations in all quantities of [Table S5](#) along the course of the
233 day in response to available sunlight are omitted from the analysis. The parameter having the
234 most uncertain value in Equation 1 is the eddy diffusion coefficient K . The value of K was
235 estimated by two independent methods, one based on Monin-Obukhov similarity theory and one
236 based on constraints from field measurements (Section S3). The two methods suggest a value of

237 K of $30 \text{ m}^2 \text{ s}^{-1}$ at the top of the canopy for the reference case of the simulation (Table S5).

238 Sensitivity studies described below address uncertainty in the estimate of K .

239 The analysis focuses on four zones of influence x_1 , x_2 , x_3 , and x_4 that respectively
240 determine 0 to 25%, 25 to 50%, 50 to 75%, and 75 to 95% of the concentration C^\dagger sampled at
241 the UAV position in the atmosphere (see also Section S2). The dagger (\dagger) symbol indicates that
242 the concentration was calculated as $\alpha = 1$ for all x . Values of x_1 , x_2 , x_3 , and x_4 represent the
243 upwind distance of each zone relative to the location of UAV sampling. A small value of x_1 , for
244 instance, corresponds to a significant influence from the emissions of the underlying and nearby
245 forest on the atmospheric concentrations sampled by the UAV. Values of x_1 , x_2 , x_3 , and x_4 are
246 obtained by (i) introducing a split boundary condition as $\alpha = 1$ for $x \leq x'$ and $\alpha = 0$ otherwise
247 and (ii) carrying out stepwise increases in x' in a series of simulations to determine 0.25 C^\dagger for x_1
248 (i.e., $x_1 = x'$ when this condition holds), 0.50 C^\dagger for x_2 , 0.75 C^\dagger for x_3 , and 0.95 C^\dagger for x_4 . Uniform
249 emissions are assumed (i.e., $\alpha = 1$ regardless of x), which differentiates the concept of zones of
250 influence from the related concept of footprint (28).

251 The obtained values of x_1 , x_2 , x_3 , and x_4 for the reference case are listed in the first row of
252 Table 1. The intervals are 0 to 150 m (x_1), 150 to 700 m (x_2), 700 to 2350 m (x_3), and 8300 m and
253 beyond (x_4). The reference case corresponds to the parameters of Table S5, and canopy wake is
254 taken into consideration. These zones of influence are represented in Figure 1 in translucent
255 overlay on the forest sub-types surrounding locations A and B of sampling in the directional
256 sector of the dominant winds (Figure S3). The plot shows that 25% of C^\dagger , represented by x_1 at the
257 first dashed line, at location A is modeled as strongly related to the emissions of the plateau
258 forest and likewise at location B to the emissions of the slope forest (see also Figure S6). For the
259 next 25% of C^\dagger , represented by x_2 at the second dashed line, there is an influence of a mixture of

260 all three forest sub-types, although the specific portions of the forest remain distinct in respect to
261 emissions traceable to locations A and B. The next 50% of C^{\dagger} until x_3 and beyond can be taken as
262 contributed by repeated forest sub-types, and the distinctness of a portion of the forest with
263 respect to its influence on location A compared to location B is nearly lost, representing an
264 average across the regional forest. For comparison, a low-flying aircraft or fixed-wing UAV
265 might have a resolution **corresponding to a** local regional average (i.e., across x_1 , x_2 , and x_3).

266 **A sensitivity analysis for different models of near-surface mixing was performed by**
267 **varying K values by 0.5 \times and 10 \times . Results are listed in Table 1 in rows 2 and 3. Increasing K**
268 **values promotes the vertical transport of VOCs (Figure S5). Even so, no significant impact of the**
269 **results on the important parameter x_1 of this study was observed (Table 1). The value of x_1 has**
270 **relatively low sensitivity across the uncertainty interval of K . This result is further consistent**
271 **with observations of vertical profiles of isoprene concentration reported in the literature, with**
272 **which there is consistency with the simulated vertical profiles for all cases in Table 1 (Figures S4**
273 **and S5).** -Additional sensitivity analyses for x_1 are presented in Table S6, and the main results do
274 not change across the range of considered uncertainties. For a central value of 150 m, x_1 varies
275 from 100 to 250 m across the sensitivity analysis. Finally, strong coherent eddies can sometimes
276 develop at the canopy edge (27, 30-32), and these coherent eddies sweep into the forest,
277 promoting the exchange of air between the forest and the overlaying atmosphere and leading to
278 strong ejections (i.e., increase K near the canopy surface). These sweep-ejection cycles extend to
279 the whole canopy on the time scale of minutes (33, 34). Without quantitative information, the
280 effects of this mechanism were investigated herein by supposing **20%** dilution of isoprene
281 concentration in the near-canopy air every 1 min. This mechanism, if active, further decreases x_1
282 to 100 m (row 4, Table 1).

283 An important aspect of the model treatment is the role of pollution because the UAV
284 sampling was conducted on the northern outskirts of Manaus. The OH concentration in the
285 reference case is representative of the chemistry of polluted conditions in central Amazonia (29).
286 Given that OH concentration was not measured in the present study, a sensitivity test was carried
287 out by decreasing the OH concentration by a factor of 3 to represent background regional
288 conditions. The value of x_1 became 500 m (row 5, Table 1). Further results are plotted in Figure
289 S5.

290 For the reference case, the ratio $C^+(15\text{ m}):C^+(47\text{ m})$ is modeled as 1.21. UAV sampling
291 was also carried out in late 2017 at height differences of 40 to 50 m over the plateau forest
292 nearby location A, and the average ratio was 1.22 (Table S7). A similar value was observed by
293 sampling at a 44-m height difference along an 80-m tall tower situated in a plateau forest about
294 100 km away for the daily period of 09:00 to 15:00 (LT) during the wet season (26). The same
295 study showed that the variability in isoprene concentrations at these altitudes over the plateau
296 forest correlated strongly with the variability in emissions from the local forest. The implication
297 of these results is that differences in sampling height over the local canopy height at location B
298 (47 m) compared to location A (15 m) are not sufficient to explain the average ratio of 1.80 in
299 isoprene concentrations, as observed herein. The increase of +80% can be partitioned
300 approximately as +20% for differences in height and +60% for differences in emissions.

301 Inversion modeling was applied to the data set collected herein to determine what
302 difference in emissions is required to sustain the observed concentration differences between
303 locations A and B. The measurements showed a difference in isoprene concentration of +60%
304 over the plateau compared to slope forest. For the reference case of the model, a difference
305 between 220% to 330% in emissions between the two forest sub-types is needed to sustain the

306 observed concentration difference. The lower estimate of 220% is obtained by assuming that the
307 emissions differences extend to the full range of x_1 and x_2 (700 m) from locations A and B
308 whereas the upper estimate of 330% is obtained by assuming that the emissions differences are
309 fully within the range of x_1 (150 m). The magnitude in differences in emissions for the different
310 forest sub-types can be rationalized by the different species compositions and environmental
311 conditions, keeping in mind the heterogeneous ecosystem of the tropical forest and the estimate
312 that 30% of trees in a tropical forest are estimated to emit isoprene (35).

313 **Atmospheric Implications**

314 Although processes at intermediate scales of several hundred meters across an ecosystem
315 are believed to exert significant control over the magnitude and type of VOC emission and
316 deposition, these processes remain incompletely understood qualitatively and less defined
317 quantitatively. Emissions models for Amazonia in particular continue to have large uncertainties,
318 including the assignment of base emission capacities, meaning the emission expected for a set of
319 standard environmental conditions. Emission capacities for various landscape types, in
320 Amazonia and elsewhere, are largely estimated by two complementary methods (36). (1) In a
321 mechanistic, bottom-up approach composition data of vegetation species for a landscape,
322 instantaneous canopy conditions at a time of interest, and plant-level functional relationships for
323 those conditions are combined to estimate landscape-scale emissions. (2) In an empirical, one-
324 size-fits-all approach canopy-level gradient or eddy flux measurements obtained for a location
325 within a landscape type are assumed to hold across the entire landscape.

326 Method 1 has worked well for temperate and boreal forests because of low species
327 diversity, and under this condition enclosure measurements of VOC emissions of the known
328 dominant plant types are possible. By comparison, method 1 has large uncertainties for tropical

329 forests because immense biodiversity in species composition challenges an accurate inventory of
330 vegetation species and emission variability among those species presents difficulties for accurate
331 functional relationships. Available literature is small relative to the forest heterogeneity. Ideally,
332 isoprene emission rates characteristic of each of these plant species apparent in Figure 2 and
333 listed in Table S1 would be known, and accurate bottom-up predictions of isoprene emissions
334 over the different sub-forests could be possible. In reality, insufficient information is available
335 and difficult to acquire, not just because of the large biodiversity but also because of the
336 dependence of emissions from a single plant on environmental conditions. In this challenging
337 context, UAV-based sample collection provides a new capability that effectively represents a
338 local, measurement-based integration kernel of emissions at intermediate scales across the
339 myriad leaf-level and plant-level factors to provide qualitatively new kinds of data sets and
340 quantify the differences in emissions of the different forest sub-types.

341 Method 2 has been successful for relatively homogeneous and open ecosystems
342 characteristic of temperate and boreal regions, and vertical profiles from towers and tethered
343 balloons have been successful in determining VOC fluxes and emissions within acceptable
344 uncertainty. For tropical forests, however, method 2, representing a single-point approach, has
345 large uncertainties because of a lack of suitable approaches for quantifying heterogeneity in
346 fluxes over scales of a kilometer or less across the landscape (37). Even locally, tower locations
347 may not be representative because a single tree next to a tower can bias the profile results,
348 especially at lower sampling heights where the small footprint contains only a few trees. In
349 Amazonia, most research towers have been located in locally elevated topographical regions
350 (i.e., plateau forests; see also Table S4), and previous emission estimates taken as representative
351 of Amazonia can have bias based on the limits of available data sets.

352 Several of the shortcomings of methods 1 and 2 applied to tropical forests can be
353 ameliorated, at least in part, by the **complementary** application of the newly emerging technology
354 of UAV-based sampling approaches. The results presented herein demonstrate the possibility of
355 UAV-based sampling to collect information efficiently at the intermediate scales across
356 footprints centered at **adjustable** longitude-latitude coordinates, as needed for understanding the
357 heterogeneity of tropical forests. Access of this type has potential for improved sampling over
358 undisturbed forests as well as over forests in forbiddingly inhospitable landscapes, such as
359 waterlogged or swampy regions. For example, as a practical matter, the VOC sampler on the
360 UAV flew from location A to location B in 5 min for sampling over two different forest sub-
361 types. As a general statement, near-canopy atmospheric measurements described in the literature
362 of tropical forest have been largely confined to a small set of locations where there are towers
363 (e.g., **Table S4**), **implying that** spatial heterogeneity has been inadequately captured. UAV
364 systems can be fully operated by powerful onboard computer controllers coordinated with a
365 satellite-based positioning system, all of which are standard on a commercial UAV such as that
366 used in this study. **Sampling with a UAV allows take-off and landing from the Earth's surface**
367 **without the presence of a tower, thus eliminating an important constraint on the site locations for**
368 **research.** Moreover, a vertically stacked multi-UAV configuration as a type of floating tower is a
369 further possibility. **Limitations must also be borne in mind, however. Current commercially**
370 **available UAVs have short flight times of < 1 h due to battery capacity and limited payload**
371 **capacity (< 10 kg), and aerospace regulations can limit flight operations in real-world practice**
372 **(ref).**

373 In summary, the presented results demonstrate intermediate-scale horizontal
374 heterogeneity of VOC concentrations, specifically isoprene concentrations, in the near-canopy

375 atmosphere over central Amazonia. Emission differences implied by the measurements are
376 quantified as 220% to 330% for the different forest sub-types across this biodiverse landscape.
377 For comparison, the state-of-the-art MEGAN model assumes homogeneity at this scale and
378 provides 0% difference in emissions between the two forest sub-types. The explanation is that
379 there has not been sufficient knowledge about horizontal heterogeneity to inform the MEGAN
380 model. These findings call attention once more to re-addressing a longstanding scientific
381 unknown related to forest heterogeneity, now in hand with newly emerging UAV-assisted
382 technical possibilities to make progress on this unknown, for understanding and quantifying
383 VOC emissions at intermediate scales to better understand the ecological and Earth system roles
384 of VOCs and to better represent them in climate and air quality model simulations.

385 **Materials and Methods**

386 **Tower.** The UAV equipped with the VOC sampler was launched and recovered from a platform
387 (3.5 m × 3.5 m) atop the MUSA tower in the Ducke Reserve. The tower corresponded to location
388 A of the study (3.0032° S, 59.9397° W; inset picture of Figure 1). Ground level was 120 m asl at
389 location A. This altitude was defined as 0 m for the reference height above ground level (rhagl)
390 for sample collection. The tower had a height of 42 m, and local forest canopy height nearby the
391 tower was 25 to 35 m. A weather station recorded wind speed and direction. Location B (2.997°
392 S, 59.936° W) was 711 m distant from the tower. Ground level was 85 m asl or -35 rhagl at
393 location B. Local canopy height at location B was also 25 to 35 m.

394 **Unmanned Aerial Vehicle.** The UAV was a DJI Matrice 600 Professional Grade. It was a
395 hexacopter design with onboard stabilization. The maximum ascent rate was 5 m s⁻¹, and the
396 maximum horizontal speed was 18 m s⁻¹. It had GPS positioning and maintained two-way

397 communication with DJI control programs deployed on a tablet computer (mini-iPad, Apple
398 Inc.). The UAV had a nominal flight time of 30 min. The VOC sampler was mounted to the
399 flight platform. Testing for the sampler mass indicated 25 min of flight time, including a margin
400 of security of an additional 5 min. Actual battery use in each flight depended on the flight plan
401 and the strength of local winds during the flight.

402 **Sampler.** The sampler mounted to the UAV was described in ref (21). In brief, samples were
403 collected by drawing air through cartridge tubes packed with Tenax TA and Carbograph 5TD
404 (C2-AXXX-5149, Markes International, Inc.; outer diameter of 6.35 mm; length of 9 cm). The
405 sorbent materials were hydrophobic and suitable for air sampling at high relative humidity (38).
406 A sample flow rate of 0.15 L min⁻¹ was used for collection. After sampling, the cartridge tubes
407 were removed from the UAV sampler, capped using Swagelok fittings outfitted with Teflon
408 ferrules (PTFE), and stored at room temperature prior to shipping to Irvine, California, USA,
409 where they were stored in a refrigerator prior to chromatographic analysis. Additional samples
410 were collected directly from the tower platform at location A using a handheld pump (GilAir
411 PLUS, Gilian) to draw air through cartridge tubes, after which they were also capped and stored
412 in the same manner.

413 **Sampling Strategy.** Sample collection times, atmospheric state variables, and isoprene and α -
414 pinene concentrations are listed in Table S2. During a UAV flight, a sampling period for a **single**
415 **cartridge was 2.5 min**. More specifically, as an example, two flights on one day between 09:00
416 and 10:00 corresponded to 5 min of sampling with **one cartridge tube**. **In the same cartridge**
417 **tube, samples were collected at the same period of the day (e.g., 09:00 to 10:00) for four days in**
418 **a week to ensure sufficient material for chemical analysis**, corresponding to 20 min or 3 L of

419 sampling for this cartridge tube (Table S2). This sampling strategy was taken to complement
420 work on semivolatile organic compounds (SVOCs; 17.5 min sampling each flight; work not
421 described herein). The strategy of sampling across a broader period also helped to average out
422 otherwise possible confounding effects of sustained downdrafts or updrafts during a single
423 sampling period. Samples were collected simultaneously over location A for 15 m above local
424 canopy and over location B for 47 m above local canopy height. The lower ground level (asl) at
425 location B required the sampling at a higher relative height above the canopy so that the UAV
426 remained in the horizontal visual field of the flight operator positioned on the tower platform at
427 location A. Although the UAV can be programmed to fly without direct operator control, this
428 option was not utilized in the present study because of evolving familiarity and confidence of the
429 researchers with the UAV technology for atmospheric applications. The influence of different
430 sampling heights was not significant enough, however, to account for observed concentration
431 differences (see main text). In all, thirty-two VOC samples were collected (4 time periods across
432 4 weeks at each location A and B).

433 **Analysis.** Thermal desorption gas chromatography was used to analyze the samples. The
434 cartridge tubes were loaded into a thermally desorbing autosampler (TD-100, Markes
435 International, Inc). **During the desorption, the tube was heated to 285 °C for 6 min with helium**
436 **carrier gas to release VOCs.** The VOCs were cryofocused at 10 °C on a cold trap and then
437 transferred **in splitless mode** to the column (30 m, DB-5) of a gas chromatograph (GC, model
438 7890B, Agilent Technologies, Inc) equipped with time-of-flight mass spectrometer (Markes
439 BenchTOF-SeV) and flame ionization detector (TD-GC-FID/TOFMS). The compounds were
440 identified by **mass** spectra and retention time and quantified by FID using authentic standards

441 (39). A multi-step temperature ramp was used for the oven from -30 °C to 260 °C. The carrier
442 gas through the column had a flow rate of 1.2 mL min⁻¹.

443 The responses to isoprene and α -pinene concentrations, which are the focus of the data
444 presentation herein, were calibrated by loading known amounts into cartridge tubes followed by
445 analysis with the same protocols as used for the atmospheric samples. The analytical system had
446 a detection limit of 1 pg for isoprene and α -pinene. The overall detection limit for the
447 atmospheric samples, however, was higher than the limit of the analytical system because the
448 background levels for cartridge tubes exposed to air (i.e., blanks) in the absence of drawn flow
449 for the corresponding time period (i.e., samples) had a typical mass loading of 10 pg. These
450 results corresponded to an approximate uncertainty in the analytical method of 2 ppt for a 3-L
451 sample. The precision was 5% (α -pinene) to 10% (isoprene). The total uncertainty was 2 ppt or
452 10%, whichever was greater. An additional uncertainty of 15% was related to the measured flow
453 of the VOC sampler. The overall combined measurement uncertainty was estimated as 20%, as
454 discussed further in ref (21).

455 **Acknowledgments:** The Manaus Botanical Gardens (MUSA) of Ducke Reserve kindly provided
456 access and logistical support. **Funding:** The Brazilian Federal Agency for Support and
457 Evaluation of Graduate Education (CAPES) (88881.187481/2018-01), the Brazilian National
458 Council for Scientific and Technological Development (CNPq), a Senior Visitor Research Grant
459 of the Amazonas State Research Foundation (FAPEAM) (062.00568/2014 and 062.00491/2016),
460 the Harvard Climate Change Solutions Fund, the Postdoctoral Program in Environmental
461 Chemistry of the Dreyfus Foundation, and the Division of Atmospheric and Geospace Sciences
462 of the USA National Science Foundation (AGS-1829025 and AGS-1829074) are acknowledged.
463 **Author contributions:** C.E.B., J.Y., R.A.F.S, and S.T.M. designed the research project. C.E.B.,
464 J.Y., I.O.B., S.D., K.J.J., A.B.G., K.A.M., L.D.M., R.A.F.S, and S.T.M. interpreted all results
465 and contributed to writing. C.E.B., J.Y., I.O.R, P.C.G., A.S.S.M., R.G.B., R.L.O., R.A.F.S, and
466 S.T.M. carried out the UAV-based sample collection. D.G. and A.B.G. performed the chemical
467 analysis. **Competing interests:** The authors declare no competing interests. **Data and materials**
468 **availability:** The experimental data and model code that support the findings of this study are
469 available from the corresponding authors upon reasonable request

470 **References**

- 471 1. Holopainen JK (2004) Multiple functions of inducible plant volatiles. *Trends Plant Sci.*
472 9(11):529-533.
- 473 2. Laothawornkitkul J, Taylor JE, Paul ND, & Hewitt CN (2009) Biogenic volatile organic
474 compounds in the Earth System. *New Phytol.* 183:27-51.

- 475 3. Guenther AB, *et al.* (2012) The model of emissions of gases and aerosols from nature
476 version 2.1 (MEGAN2.1): an extended and updated framework for modeling biogenic
477 emissions. *Geosci. Model Dev.* 5(6):1471-1492.
- 478 4. Malhi Y, *et al.* (2002) An international network to monitor the structure, composition and
479 dynamics of Amazonian forests (RAINFOR). *J. Veg. Sci.* 13(3):439-450.
- 480 5. ter Steege H, *et al.* (2013) Hyperdominance in the Amazonian tree flora. *Science*
481 342(6156):1243092.
- 482 6. Laurance WF, *et al.* (2004) Pervasive alteration of tree communities in undisturbed
483 Amazonian forests. *Nature* 428(6979):171-175.
- 484 7. Myster RW ed (2017) *Forest structure, function and dynamics in Western Amazonia*
485 (Wiley, New York), p 206.
- 486 8. Kaser L, *et al.* (2015) Chemistry-turbulence interactions and mesoscale variability
487 influence the cleansing efficiency of the atmosphere. *Geophys. Res. Lett.* 42(24):10,894-
488 810,903.
- 489 9. Butler T, *et al.* (2008) Improved simulation of isoprene oxidation chemistry with the
490 ECHAM5/MESSy chemistry-climate model: lessons from the GABRIEL airborne field
491 campaign. *Atmos. Chem. Phys.* 8(16):4529-4546.
- 492 10. Auger L & Legras B (2007) Chemical segregation by heterogeneous emissions. *Atmos.*
493 *Environ.* 41(11):2303-2318.
- 494 11. Krol MC, Molemaker MJ, & de Arellano JVG (2000) Effects of turbulence and
495 heterogeneous emissions on photochemically active species in the convective boundary
496 layer. *J. Geophys. Res. Atmos.* 105(D5):6871-6884.

- 497 12. Ouwersloot H, *et al.* (2011) On the segregation of chemical species in a clear boundary
498 layer over heterogeneous land surfaces. *Atmos. Chem. Phys.* 11(20):10681-10704.
- 499 13. Ribeiro JELdS, *et al.* (1999) *Flora da Reserva Ducke : guia de identificação das plantas*
500 *vasculares de uma floresta de terra-firme na Amazônia Central* (INPA, Manaus) p 799.
- 501 14. Schiatti J, *et al.* (2013) Vertical distance from drainage drives floristic composition
502 changes in an Amazonian rainforest. *Plant Ecol. Divers.* 7(1-2):241-253.
- 503 15. Oliveira ANd, *et al.* (2008) Composição e diversidade florístico-estrutural de um hectare
504 de floresta densa de terra firme na Amazônia Central, Amazonas, Brasil (Translation:
505 Composition and floristic-structural diversity of one hectare of dense terra firme forest in
506 Central Amazonia, Amazonas, Brazil). *Acta Amaz.* 38:627-641.
- 507 16. Cardoso D, *et al.* (2017) Amazon plant diversity revealed by a taxonomically verified
508 species list. *Proc. Natl. Acad. Sci.* 114(40):10695-10700.
- 509 17. Sindelarova K, *et al.* (2014) Global data set of biogenic VOC emissions calculated by the
510 MEGAN model over the last 30 years. *Atmos. Chem. Phys.* 14(17):9317-9341.
- 511 18. Villa T, Gonzalez F, Miljievic B, Ristovski Z, & Morawska L (2016) An overview of
512 small unmanned aerial vehicles for air quality measurements: present applications and
513 future perspectives. *Sensors* 16(7):1072.
- 514 **19. Oliveira ML, Baccaro F, Braga-Neto R, & Magnusson WE (2008) *Reserva Ducke: a***
515 ***biodiversidade Amazônica através de uma grade (Translation: Ducke Reserve: the***
516 ***Amazonian biodiversity through a grid) (Áttema Design Editorial, Manaus) p 170.***
- 517 20. Ribeiro JELS, Nelson BW, Silva MFd, Martins LSS, & Hopkins M (1994) Reserva
518 florestal ducke: diversidade e composição da flora vascular. *Acta Amaz.* 24(1-2):19-30.

- 519 21. McKinney KA, *et al.* (submitted) A sampler for atmospheric volatile organic compounds
520 by copter unmanned aerial vehicles. *Atmos. Meas. Tech.*
- 521 22. Jardine KJ, *et al.* (2015) Green leaf volatile emissions during high temperature and
522 drought stress in a central amazon rainforest. *Plants* 4(3):678-690.
- 523 23. Alfonsi G (2009) Reynolds-averaged navier–stokes equations for turbulence modeling.
524 *Appl. Mech. Rev.* 62(4):040802.
- 525 24. Lenschow D (1995) Micrometeorological techniques for measuring biosphere-
526 atmosphere trace gas exchange. *Biogenic Trace Gases: Measuring Emissions from Soil
527 and Water*:126-163.
- 528 25. Kuhn U, *et al.* (2007) Isoprene and monoterpene fluxes from Central Amazonian
529 rainforest inferred from tower-based and airborne measurements, and implications on the
530 atmospheric chemistry and the local carbon budget. *Atmos. Chem. Phys.* 7(11):2855-
531 2879.
- 532 26. Yáñez-Serrano AM, *et al.* (2015) Diel and seasonal changes of biogenic volatile organic
533 compounds within and above an Amazonian rainforest. *Atmos. Chem. Phys.* 15(6):3359-
534 3378.
- 535 27. Finnigan J (2000) Turbulence in plant canopies. *Annu. Rev. Fluid Mech.* 32(1):519-571.
- 536 28. Lin J, *et al.* (2003) A near-field tool for simulating the upstream influence of atmospheric
537 observations: The Stochastic Time-Inverted Lagrangian Transport (STILT) model. *J.
538 Geophys. Res. Atmos.* 108(D16), 4493.
- 539 29. Martin S, *et al.* (2017) The Green Ocean Amazon experiment (GoAmazon2014/5)
540 observes pollution affecting gases, aerosols, clouds, and rainfall over the rain forest. *Bull.
541 Am. Meteorol. Soc.* 98(5):981-997.

- 542 30. Fuentes JD, *et al.* (2016) Linking meteorology, turbulence, and air chemistry in the
543 Amazon rain forest. *Bull. Am. Meteorol. Soc.* 97(12):2329-2342.
- 544 31. Raupach M & Thom AS (1981) Turbulence in and above plant canopies. *Ann. Rev. Fluid*
545 *Mech.* 13(1):97-129.
- 546 32. Raupach MR & Shaw R (1982) Averaging procedures for flow within vegetation
547 canopies. *Bound. Layer Meteorol.* 22(1):79-90.
- 548 33. Katul G, Porporato A, Cava D, & Siqueira M (2006) An analysis of intermittency,
549 scaling, and surface renewal in atmospheric surface layer turbulence. *Physica D*
550 215(2):117-126.
- 551 34. Robinson SK (1991) Coherent motions in the turbulent boundary layer. *Ann. Rev. Fluid*
552 *Mech.* 23(1):601-639.
- 553 35. Harley P, *et al.* (2004) Variation in potential for isoprene emissions among Neotropical
554 forest sites. *Glob. Change Biol.* 10(5):630-650.
- 555 36. Guenther A, *et al.* (2006) Estimates of global terrestrial isoprene emissions using
556 MEGAN (Model of Emissions of Gases and Aerosols from Nature). *Atmos. Chem. Phys.*
557 6(11):3181-3210.
- 558 37. Misztal PK, *et al.* (2016) Evaluation of regional isoprene emission factors and modeled
559 fluxes in California. *Atmos. Chem. Phys.* 16(15):9611-9628.
- 560 38. Brown VM, Crump DR, Plant NT, & Pengelly I (2014) Evaluation of the stability of a
561 mixture of volatile organic compounds on sorbents for the determination of emissions
562 from indoor materials and products using thermal desorption/gas chromatography/mass
563 spectrometry. *J. Chromatogr. A* 1350:1-9.

564 39. Faiola C, Erickson M, Fricaud V, Jobson B, & VanReken T (2012) Quantification of
565 biogenic volatile organic compounds with a flame ionization detector using the effective
566 carbon number concept. *Atmos. Meas. Tech.* 5(8):1911-1923.

567

568 **Table 1.** Sensitivity analysis for different models of near-surface mixing. For each case, the
569 distances x_1 , x_2 , x_3 , and x_4 for the zones of influence are listed. *Table S5 presents values
570 used in the reference case. ** Gradient from 30 to 10 $\text{m}^2 \text{s}^{-1}$ from canopy to $3h$ and 10 m^2
571 s^{-1} for $>3h$. Canopy height h varied from 25 to 35 m at the sampling locations.
572 ***Noontime hydroxyl radical concentration of $2.0 \times 10^{12} \text{ molec m}^{-3}$ for background
573 conditions (ref).

Physical or chemical processes	Eddy diffusion coefficient $K (\text{m}^2 \text{s}^{-1})$	VOC species	Lifetime τ against reactive loss (s)	Zones of Influence			
				x_1 (m)	x_2 (m)	x_3 (m)	x_4 (m)
				Reference case* (Polluted)	30 to 10 $\text{m}^2 \text{s}^{-1}$; 10 $\text{m}^2 \text{s}^{-1}$ **	isoprene	1630
Polluted	15 to 5 $\text{m}^2 \text{s}^{-1}$; 5 $\text{m}^2 \text{s}^{-1}$	isoprene	1630	150	650	2250	7750
Polluted	300 to 100 $\text{m}^2 \text{s}^{-1}$; 100 $\text{m}^2 \text{s}^{-1}$	as above	as above	150	950	3300	11850
Polluted + Sweep-Ejection (20% dilution)	30 to 10 $\text{m}^2 \text{s}^{-1}$; 10 $\text{m}^2 \text{s}^{-1}$	as above	as above	100	450	1550	6350
Background regional conditions***	as above	as above	4900	500	2950	10350	33400

574

575 **List of Figures**

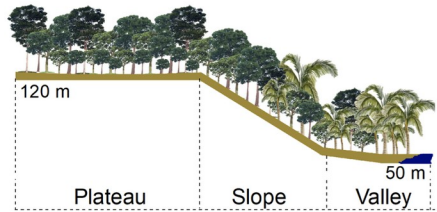
576 **Figure 1.** Local topography surrounding the tower (location A) at the Manaus Botanical
577 Gardens (“MUSA”) of the Adolfo Ducke Forest Reserve in the central Amazon,
578 Brazil. The UAV flight route from location A over the plateau forest to location B
579 over the slope forest is shown by the red line. Zones of influence are shown in
580 translucent overlay on the forest sub-types surrounding locations A and B (**Figure**
581 **S6**). **The sector angle of each translucent overlay represents the variability of wind**
582 **direction in the steady trade winds during the period of study. The dashed arc lines**
583 **within a sector represent transitions from one zone of influence x_i to the next.**

584 **Figure 2.** Photographs of the trees of the plateau forest (location A) and the slope forest
585 (location B) of Figure 1. The downward images on the left of the top of the forest
586 canopy were taken by a camera on the UAV. The upward images on the right from
587 the ground through the canopy were taken by a hiker at those locations.

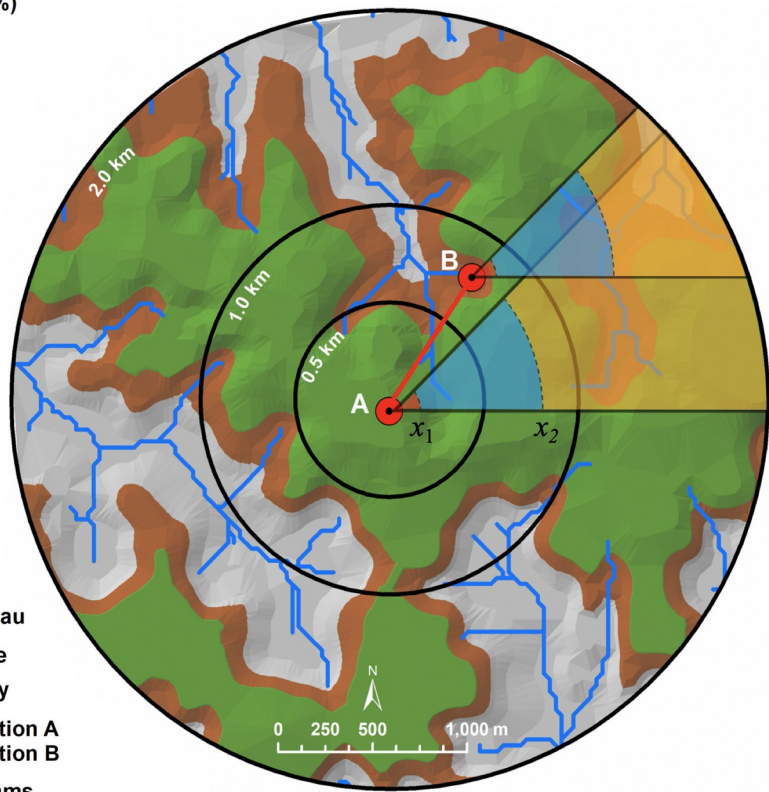
588 **Figure 3.** Isoprene-to- α -pinene concentration ratios measured during morning hours. (**green**)
589 Over the plateau forest for 15 m above local canopy height at location A of Figure 1.
590 (**orange**) Over the slope forest for 47 m above local canopy height at location B.
591 Panels A, B, C, and D represent weeks 1, 2, 3, and 4, respectively, of the
592 measurement period.

593

Area Radius	Plateau (%)	Slope (%)	Valley (%)
0.5 km	95	5	0
1 km	66	19	15
2 km	49	24	27



Typical relief at study area (above sea level)



- Plateau
- Slope
- Valley
- Location A
- Location B
- Streams
- UAV route

594

595 **Figure 1**

596

597 (a) Plateau forest



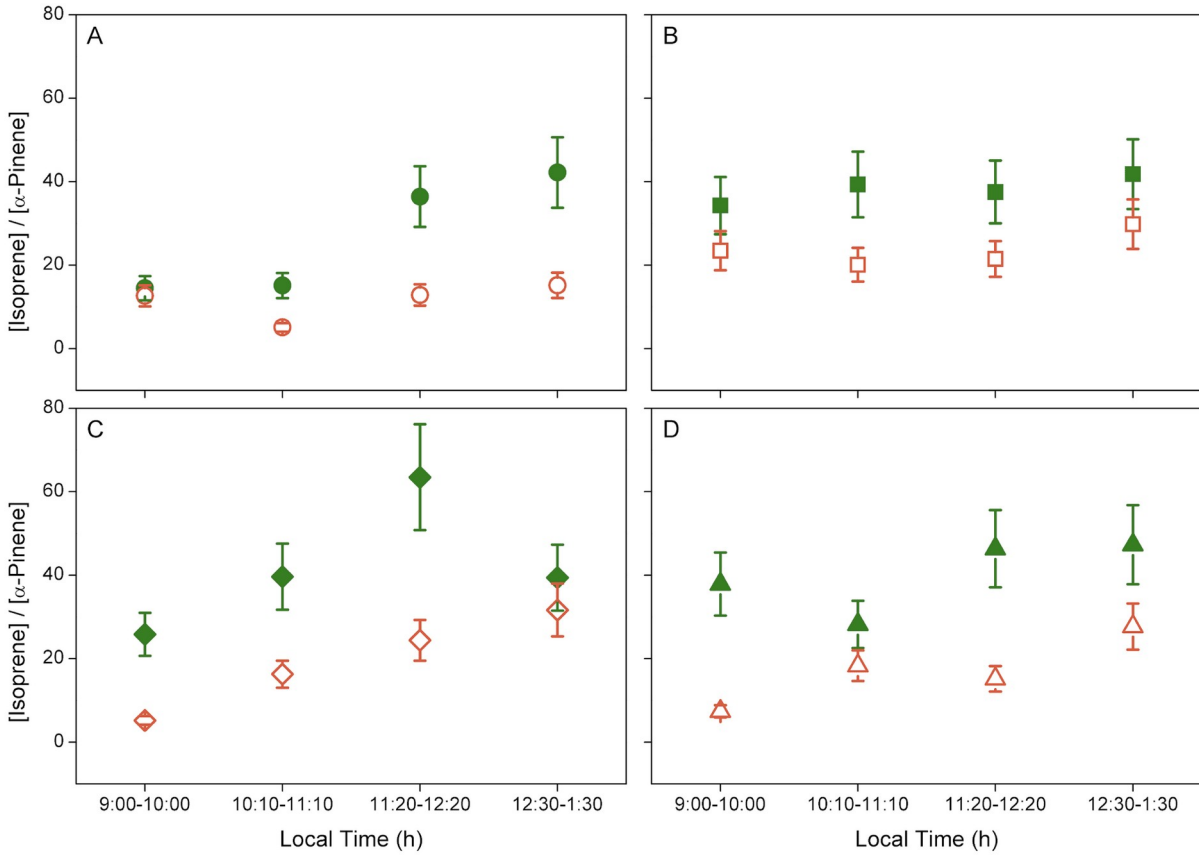
598
599 (b) Slope forest



600

601 **Figure 2**

602



603

604 **Figure 3**

605